Computation of Corrective Control Actions to Prevent Dynamic Voltage Instability

Thomas J. Overbye
Department of Electrical and Computer Engineering
University of Illinois at Urbana-Champaign
Urbana, IL 61801

Abstract

One of the mechanisms by which dynamic voltage instability can originate is through the occurrence of a contingency which causes the system to lose its equilibrium point. In this context the static power flow equations would become unsolvable. If corrective control action is not taken quickly enough following the contingency, the system state will vary as dictated by system dynamics with the usual consequence of voltage collapse. This paper presents a method to determine these corrective control actions, with particular attention given to determining the allowable time frame for corrective control. To this end, a structure-preserving energy function is used to define a potential energy well in voltage space for the post-control system, with the stable equilibrium point corresponding to the bottom of the well, while unstable equilibrium points correspond to saddle points on the boundary of the well. Then a sufficient condition for the system to retain stability following the contingency is that the corrective control action be completed before the system state has gained sufficient energy to escape the well. The paper addresses the practical considerations of applying this method to a realistically sized system which contain a large number of potential controls. The method is demonstrated on both small systems and the IEEE 118 bus test system.

I. Introduction

Optimal transmission system operation requires adequate control strategies for the prevention of voltage instability. The lack of such strategies can result in either a widespread blackout due to voltage collapse, or more commonly, unduly constrained system economic operation to avoid an imprecisely defined threat of voltage instability. Voltage instability generally arises from two types of system events: gradual parameter variation (such as due to load/generation variation), and contingencies. In the first case the system state is assumed to move from a point of relative security to one of increased vulnerability to voltage instability through a quasi-static variation (time scale of tens of minutes to hours). The system then ultimately experiences voltage collapse as a result of either a saddle node bifurcation in which the system's operating equilibrium disappears [1], or as the result of a Hopf bifurcation in which a pair of eigenvalues of the system Jacobian cross the imaginary axis with nonzero imaginary part [2].

In the second case, a previously stable system loses voltage stability due to the occurrence of a large disturbance, such as a line outage contingency. Then, in the absence of effective control intervention, the system would eventually experience voltage collapse. For such a case there are three mechanisms by which the system could experience collapse. First, the system has an equilibrium point but it is unstable. Second, following the contingency the system does not have an equilibrium point. Mathematically this corresponds to lack of a real solution to the power flow equations. Third, a stable equilibrium exists, but following the contingency the system state is not within the region of attraction (ROA) of this equilibrium. This paper will be primarily concerned with developing control strategies for dealing with the second and, to some extent, the third possibilities.

The paper is organized as follows. First, the static measure from [3] for quantifying the unsolvability of such power flow cases, along with the method from [4] for developing statically optimal control responses to restore such a case to solvability are reviewed. Then, the full dynamic consequences of unsolvability are considered. The method is demonstrated on both small systems and the IEEE 118 bus system.

II. Static Considerations of Unsolvability

As is known to most planning and operations engineers, there are often contingent (or sometimes basecase) situations for which the Newton-Raphson (N-R) power flow does not converge. Since convergence is not guaranteed, this situation could be due to either a poor initial voltage guess, or because the case does not have a real solution. Examples of the former can be reduced through various methods to prevent power flow divergence. The concern in this paper is with the later. This section reviews a Euclidean measure to quantify the unsolvability of such cases, and a method to compute the statically optimal control responses to restore the case to solvability [3], [4].

Consider the two bus system shown in Figure 1, where bus 1 is the slack bus and bus 2 is a load bus. The buses are connected through the two transmission lines as shown with the indicated per unit reactances (100 MVA base). The system power flow equations can then be written as

$$S = f(x) \tag{1}$$

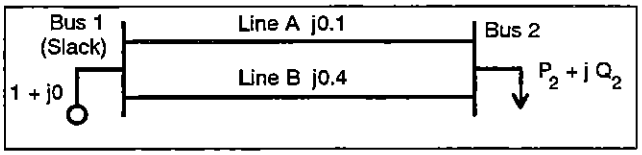

Figure 1: Two Bus System

where S is a vector of the constant real and reactive power load minus generation at all buses except the slack

$$S = [P_2, Q_2]^T \quad (2)$$

x is the nonslack bus voltage vector in rectangular notation, $V_i = e_i + jf_i$,

$$x = [e_2, f_2]^T \quad (3)$$

f is the function of the real and reactive power balance constraints

$$f = [f_{p2}(x), f_{q2}(x)]^T \quad (4)$$

$$f_{pi}(x) = - \sum_{j=1}^{n} [e_i(e_jG_{ij} - f_jB_{ij}) + f_i(f_jG_{ij} + e_jB_{ij})] \quad (5a)$$

$$f_{qi}(x) = - \sum_{j=1}^{n} [f_i(e_jG_{ij} - f_jB_{ij}) - e_i(f_jG_{ij} + e_jB_{ij})] \quad (5b)$$

and G + jB is the network bus admittance matrix.

Depending upon the values of P_2 and Q_2, the power flow equations (1) can have either two, one, or no real solutions [5]. The region in load parameter space with two solutions is defined as the solvable region, while the region with no solution is defined as the unsolvable region; the two regions are separated by a hypersurface Σ where the equations have a single solution and upon which the Jacobian of (4) is singular.

The boundary Σ is dependent, of course, upon the system topology. For example, Figure 2 shows this boundary in load parameter space for the two bus basecase with a constant power load S of 500 MW and 100 Mvar (dashed line), and for a contingent case with line B removed (solid line). Note that the contingency has caused the operating point to change from being within the solvable region to the unsolvable region. The problem then is to first quantify the unsolvability of the case, and then to determine the optimal method to return to solvability.

The unsolvability of the case can be quantified using the Euclidean distance in load parameter space from the point S (in the unsolvable region) to the closest point on the boundary Σ. This closest boundary point is determined by first defining a cost function of one half the square of the power flow mismatch equations:

$$F(x) = \frac{1}{2} [f(x) - S]^T [f(x) - S] \quad (6)$$

Note that F(x) is greater than or equal to zero for all x, and is equal to zero only at the power flow solutions.

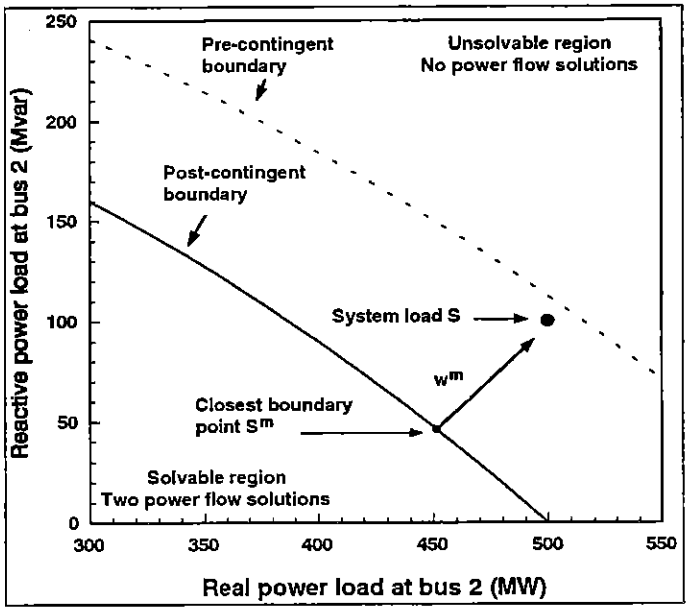

Figure 2 : P_2/Q_2 Parameter Space Relationships

Since the case is unsolvable, there is no x such that F(x) = 0. Rather, let x^m be defined as the value of x corresponding to the minimum of the cost function F(x); thus x^m can be thought of as the "best possible" solution to the power flow equations. Define $S^m = f(x^m)$ to be the point in parameter space corresponding to x^m. In [3] it is shown that S^m is the closest point on Σ to S. The Euclidean distance between these points, given by:

$$\beta = \| S^m - S \| = \sqrt{[S^m - S]^T [S^m - S]} \quad (7)$$

is then used to measure the unsolvability of S. A power flow based algorithm to determine x^m and hence S^m is presented in [3]. As an example, for the two bus case the closest boundary point is determined to be 451.4/46.2 MW/Mvar with β = 0.725 per unit (see Figure 2); at this point $x^m = [0.500\ -0.451]^T$.

The direction in parameter space to the closest boundary point is then just $-[S - S^m]$, which is parallel to the normal vector of Σ at S^m. At S^m the Jacobian of $f(x^m)$, $J(x^m)$, has (generically) a single zero eigenvalue. In [6], [7] it is shown that the left eigenvector associated with the zero eigenvalue of $J(x^m)$, w^m, is parallel to the normal vector to Σ at S^m.

Since S is an element of the normal ray emanating from S^m, the "optimal" direction (at least in a Euclidean sense) to move back to Σ is in the opposite direction to the normal, that is $[S - S^m]$. However this direction is seldom practical since it commonly involves changes in power injections at a large percentage of system buses, and in its determination neither cost not the availability of such controls has been considered. Rather, to calculate the sensitivity of β to practical controls, let u be defined as the vector of such controls. Then, using a result from [7], the sensitivities of β with respect to u are given by

$$\beta_u = -w^m [f(x^m) - S]_u \quad (8)$$

where $[f(x^m) - S]_u$ is the Jacobian of the power flow equations with respect to the system controls u, and w^m is the normalized left eigenvector associated with the zero eigenvalue of $J(x^m)$. The sign ambiguity of the eigenvector w^m (outward or inward from Σ) is resolved by choosing it to always be directed outward (i.e., sign of w^m is chosen so that $(S - S^m) \cdot w^m > 0$).

The values of β_u then provide a linear estimate of the effect a particular control has upon β. Neglecting nonlinearities, the necessary change in a single control u_i to just return the case to solvability is given by $-\beta/\beta_{u_i}$. For the case of power injection controls (i.e., elements of S), for which $[f(x^m) - S]_{u_i}$ (the column of the Jacobian corresponding to u_i) is constant, the accuracy of the linearization depends only upon the distance of S from Σ and the curvature of Σ in the vicinity of S^m. The error is the difference between Σ and its tangent plane approximation at S^m. For other controls the linearization accuracy also depends upon how well $[f(x^m) - S]$ is approximated by the Jacobian linearization.

As an example, Table 1 compares the estimated and actual changes needed for different controls to return the two bus case to solvability. Which control(s) to use depends upon their relative cost and availability, with the switching in of shunt capacitance being undoubtedly preferable to shedding load. The last line in the table represents the more realistic load shed scenario in which both real and reactive power are simultaneously shed to maintain the same power factor (in this case pf = 0.98). Of course one would usually want to move the control by more than the actual value given in the table to provide a margin of security. The effects of these load controls in load parameter space are shown in Figure 3. There is of course nothing in the method which would preclude using multiple controls simultaneously. Additonally, application of the method to larger systems is straightforward, and because of the sparsity of $[f(x^m) - S]_u$, the sensitivities can be computed with minimal computation. More details and an example using the IEEE 118 bus system are contained in [4].

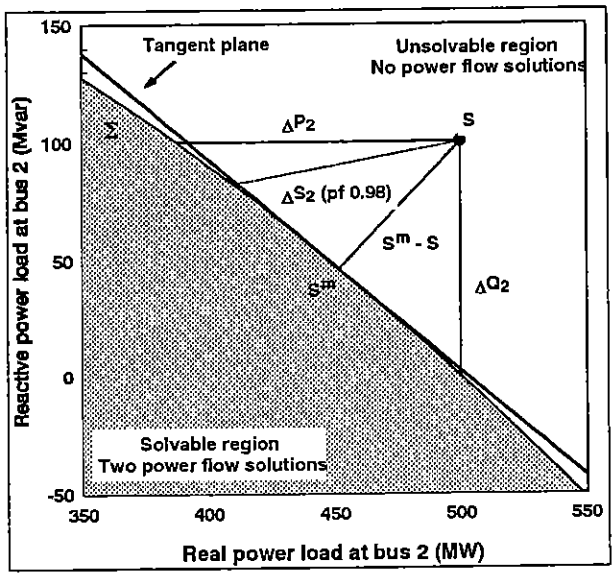

Figure 3 : Load Changes to Return Case to Solvability

	P = 5.0, Q = 1.0 (per unit), β = 0.725		
Control (per unit)	Estimate	Actual	% Error
ΔC_2	2.15	1.80	16.3
ΔP_2	-1.082	-1.127	4.0
ΔQ_2	-0.976	-1.000	2.5
ΔS_2 (0.98 pf)	-0.904	-0.922	2.0

Table 1 : Two Bus Control Changes to Return to Solvability

III. Dynamic Considerations of Unsolvability

The previous section examined the unsolvable power flow problem using purely static analysis. However to fully consider this problem, the dynamic consequences of the loss of the power flow solution must also be addressed. The unsolvable power flow problem is, by definition, one for which the system dynamic equations no longer have an equilibrium point. Thus, if control action is not taken sufficiently quickly following the contingency which pushed the system into the unsolvable state, the system would typically experience voltage instability and eventual collapse.

Thus a method is needed to determine how quickly the controls must be applied to avoid voltage collapse. This information could then be used to determine if the proposed controls possess the necessary time rate of response. A practical example of this situation is mentioned in [8], where, in order to avoid voltage collapse, utilities need to decide between installing fast and expensive SVC's, or the more inexpensive but slower switched capacitors. Note that this problem is akin to the transient stability problem in which the question is to determine how quickly a control (typically circuit breaker operation to clear a fault) must be applied to avoid angular instability. The main difference between these two problems is the much shorter time frame for the transient stability problem.

To study the dynamic consequences of unsolvability, the static power flow equations need to be augmented to include system dynamics. This will be done initially by just considering load dynamics, with generators represented using the standard power flow PV bus model (i.e., constant real power and voltage magnitude) provided their reactive power is within limits, and by the PQ bus model if the reactive output attempts to exceed these limits. A number of different dynamic load models have been proposed, with one popular model motivated by the fact that many loads are equipped with regulators (including down-stream LTC transformers) which, when modeled in aggregate, vary the load according to a generic first order model [8], [9], [10], [11], [12]:

$$T_{pi}\dot{\lambda}_{pi} = P_{oi}V_i^a - \lambda_{pi}V_i^\alpha := \Delta P_i(x) \qquad (9a)$$

$$T_{qi}\dot{\lambda}_{qi} = Q_{oi}V_i^b - \lambda_{qi}V_i^\beta := \Delta Q_i(x) \qquad (9b)$$

with $T_{pi}, T_{qi} > 0$. The first term on the right-hand side represents the static load demand at the bus, while the second term is the dynamic load demand. A necessary condition for

an equilibrium point is that the static demand equal the dynamic demand. During the course of a dynamic simulation, the dynamic power balance equations must always be satisfied:

$$\lambda_{pi} V_i^{\alpha} - f_{pi}(\mathbf{x}) = 0 \quad (10a)$$

$$\lambda_{qi} V_i^{\beta} - f_{qi}(\mathbf{x}) = 0 \quad (10b)$$

where $\mathbf{x}$ is the vector of the voltage angles at all system buses (except the slack) and the voltage magnitudes at all buses except the PV generator buses ($\mathbf{x}$ is now expressed in polar coordinates for better clarity of system dynamics). At buses with no dynamic load (such as buses with no load, PV generator buses, or purely static load buses) the values of λ_{pi} and λ_{qi} are constant, and the steady state load demand is identical to the dynamic load demand:

$$P_{oi} V_i^{a} = \lambda_{pi} V_i^{\alpha} \quad (11a)$$

$$Q_{oi} V_i^{b} = \lambda_{qi} V_i^{\beta} \quad (11b)$$

At all other buses λ varies according to (9) in an attempt to reach an equilibrium point.

To illustrate this problem, again consider the two bus case, but with line B's impedance changed to j0.1. Using the load model from (9), let $P_{o2} = 5.0$, $Q_{o2} = 1.0$, a=0, b=0, α=2, β=2, and $T_{p2} = T_{q2} = 5$ seconds. From Table 1 it is seen that following the outage of line B the case would be unsolvable, with $\beta = 0.725$. At some point after the line outage assume a 220 Mvar shunt capacitor is switched in at the load bus. The Table 1 results show that from a purely static point of view this should be sufficient restore solvability. Since the static load demand has no voltage dependence (i.e., a and b are zero), the desired equilibrium point $\mathbf{x}^s$ is the power flow solution after the capacitor has been inserted; the load bus voltage of this solution is $0.962\angle -31.3°$. The actual dynamic response of the load bus voltage magnitude is shown in Figure 4 for different capacitor switching times. As was shown in [8] and in this figure, it is clear that the time of control application is of critical importance to whether the system eventually reaches the equilibrium $\mathbf{x}^s$.

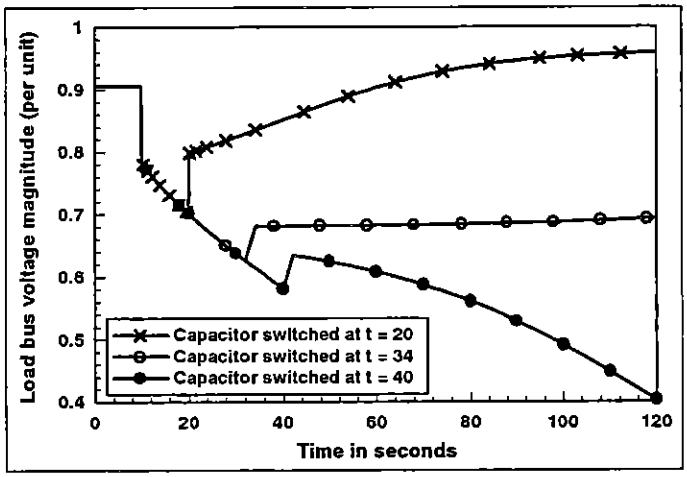

Figure 4 : Load Bus Voltage for Different Switching Times

The traditional method of solving this type of problem is to perform a series of computationally expensive time domain simulations. This is necessary because while each simulation can determine whether a case is stable or not, it does little to quantify the degree of stability. In contrast, energy function methods provide a direct means to quantify system stability. The use of energy function methods for the related problem of transient stability is well documented [13], [14], while their use for quasi-static voltage stability is more recent [15], [16]. Since the present problem combines aspects of both, this suggests the use of a unified energy framework [17].

Using the structure-preserving energy function from [15], $\vartheta(\mathbf{x})$, define a "potential energy well" in voltage space for the system after controls have been applied (i.e., the post-control system). The SEP (high voltage power flow solution) $\mathbf{x}^s$ corresponds to the bottom of the well, while a subset of the UEPs (low voltage power flow solutions) correspond to saddle points on the boundary of the well. Then, provided the energy derivative along trajectories of the system, $\dot{\vartheta}(\mathbf{x})$, is less than or equal to zero within a bounded region Ω_c about $\mathbf{x}^s$, a sufficient condition for the system to retain stability following the contingency is that the control action be completed before the system has gained sufficient energy to escape the well, with the minimum value equal to the energy of a low voltage solution on the boundary of the well, defined as ϑ^{cr}. The region Ω_c is defined as the set of all $\mathbf{x}$ about $\mathbf{x}^s$ for which $\vartheta(\mathbf{x}) < \vartheta^{cr}$. For $\vartheta(\mathbf{x})$ to formally define a Lyapunov function some restrictions would need to be placed on system models, including not allowing voltage dependence in $P_s(V)$ and restricting the method to networks with no transfer conductance terms. In the realistic systems considered here, these restrictions are relaxed, and the term "energy function" is used rather than Lyapunov function.

Before applying energy methods to the problem, it is necessary to develop conditions for the load model from (9) such that $\dot{\vartheta}(\mathbf{x}) \leq 0$ for $\mathbf{x} \in \Omega_c$ This is done by first developing the relationship between $\mathbf{x}$ and λ. By dividing both sides of (10a) by V_i^{α} and (10b) by V_i^{β}, λ can be written as an explicit function of $\mathbf{x}$:

$$\lambda = g(\mathbf{x}) \quad (12)$$

from which it is straightforward to show that

$$\dot{\lambda} = J(\mathbf{x})\,\dot{\mathbf{x}} \quad (13)$$

$$\dot{\mathbf{x}} = J(\mathbf{x})^{-1}\,\dot{\lambda} \quad (14)$$

where $J(\mathbf{x})$ is the Jacobian of $g(\mathbf{x})$. Also recall the definition of the energy derivative

$$\dot{\vartheta}(\mathbf{x}) = \nabla\vartheta(\mathbf{x})\,\dot{\mathbf{x}} \quad (15)$$

and that for $\vartheta(\mathbf{x})$ from [15] (with a lossless system) for the post-control system

$$\nabla\vartheta(\mathbf{x}) = [\Delta P(\mathbf{x}) \quad \Delta\tilde{Q}(\mathbf{x})] \quad (16)$$

where $\Delta\tilde{Q}_i(x) = \Delta Q_i(x) / V^i$. Then using (14) and (9) we get

$$\dot{x} = J(x)^{-1} \begin{bmatrix} \frac{V^\alpha}{T_p} & 0 \\ 0 & \frac{V^{\beta+1}}{T_q} \end{bmatrix} \begin{bmatrix} \Delta P(x) \\ \Delta\tilde{Q}(x) \end{bmatrix} \quad (17)$$

Finally, defining the diagonal matrix as A, $\dot{\vartheta}(x)$ can then be rewritten as

$$\dot{\vartheta}(x) = [\Delta P(x) \quad \Delta\tilde{Q}(x)] \, J(x)^{-1} A \begin{bmatrix} \Delta P(x) \\ \Delta\tilde{Q}(x) \end{bmatrix} \quad (18)$$

A sufficient condition for $\dot{\vartheta}(x) \le 0$ is that $J(x)^{-1}A$ be negative definite. Whether this condition is met depends both upon $J(x)$ and A. For the case where all the time constants T_{pi} and T_{qi} are identical (i.e., $A = \alpha I$ with α equal to the time constant), this condition is met if all of the eigenvalues of $0.5 (J(x) + J(x)^T)$ are negative. Otherwise the condition depends upon the relative values of T_{pi} and T_{qi}; it is strongly dependent upon the ratio of these two values at a particular bus i. In actuality the size of the region about x^s for which $\dot{\vartheta}(x) \le 0$ is typically larger than that for which $J(x)^{-1}A$ is negative definite. This is due to constraints on allowable values of $[\Delta P(x) \; \Delta\tilde{Q}(x)]$ imposed by (9) and (10). The size of the region for which $J(x)$ is negative definite depends upon the load parameters α_i and β_i with, in general, the region enlarging for higher values. Numerical testing indicates that for realistic load models the condition that $\dot{\vartheta}(x) \le 0$ is usually met along system trajectories.

The maximum time to apply control following a contingency is then determined by calculating the energy for the contingent system trajectory assuming no control action (analogous to the transient stability fault-on trajectory). Since this system has no equilibrium point, the system will eventually gain sufficient energy to exit the region of attraction about x^s. The time at which $\vartheta(x)$ increases to ϑ^{cr} is then the critical time -- control must be applied before this time to guarantee stability. For example Figure 5 shows the contours of the post-control energy well for the two bus case, with the SEP at 0.962 ∠-31.3° and the UEP at 0.679∠-47.4°;

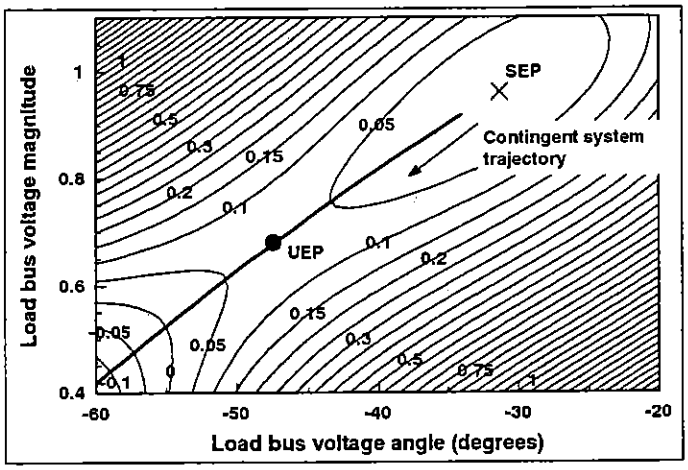

Figure 5 : Two Bus System Energy Well

the energy associated with the low voltage solution saddle node is $\vartheta^{cr} = 0.0593$. Superimposed on the well is the contingent system trajectory assuming no control action. To retain stability, the capacitor must be switched in before the trajectory exits the region of attraction of SEP. For this case, in which the trajectory passes almost through the UEP, the critical switching time is when the energy is equal to that of the UEP. Figure 6 plots the value of this energy as a function of time. From the figure it is directly seen that the trajectory passes through this point at about 34 seconds. The result demonstrating the switching of the capacitor at this critical time is shown by the second curve in Figure 4.

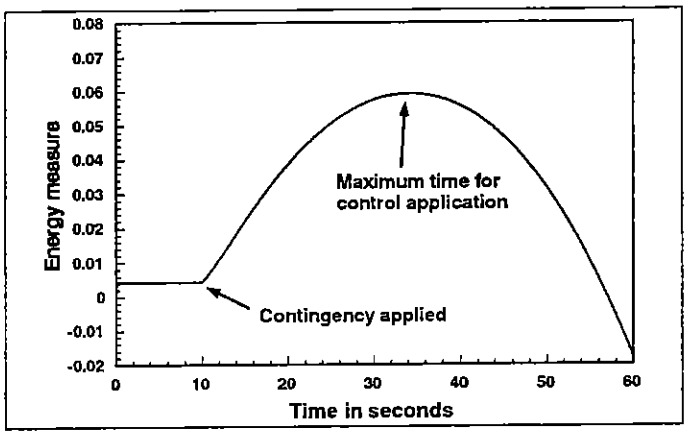

Figure 6 : Contingent System Energy with No Control

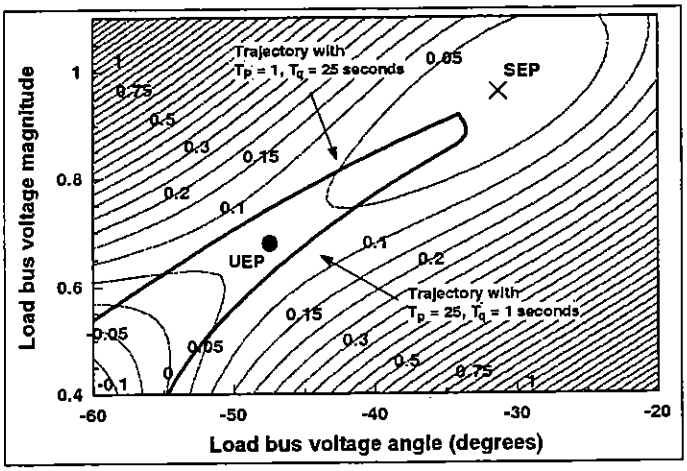

Figure 7 : Two Bus System Trajectories

The point at which the trajectory exits the region of attraction of the SEP is dependent of course on T_{pi} and T_{qi}. Figure 7 shows the two bus trajectories first for a case in which the reactive power responses much faster than the real power (lower trajectory in the figure), and then for the opposite case (upper trajectory). Note that the trajectories no longer exit through the UEP. Similar to the transient stability problem, there are two choices for the critical energy value: the energy associated with the controlling UEP [18], or the potential energy boundary surface method (PEBS) which determines the maximum potential energy along the uncontrolled system trajectory [19]. For the first trajectory the UEP method estimates a maximum control time of 85

seconds, while the PEBS methods gives 127 seconds. The actual time is 115 seconds. For the second trajectory the UEP method estimates a maximum control time of 13.1 seconds, while the PEBS method gives 16.1 seconds. The actual for this case is 20.4 seconds. This discrepancy arises because the wide ratios in the time constants result in a situation where $\dot{\vartheta}(x)$ actually becomes positive slightly after the trajectory has passed through the PEBS.

To demonstrate the method on a system with more than a single UEP, consider the three bus system shown in Figure 8. For a contingency resulting in the loss of one of the lines from bus 2 to bus 3 the case becomes unsolvable with β = 0.09. One method to restore solvability is to switch in both of the 100 Mvar capacitor banks at buses 1 and 2. The post-control system then has the SEP solution shown in Table 2, along with three UEP solutions. UEPs A and B are type-one solutions, while UEP C is type-two. How quickly the capacitors must be switched depends upon the load model. Assume that the loads are modeled using the dynamic model from (9) with a=0, b=0, α=2, β=2 at both buses.

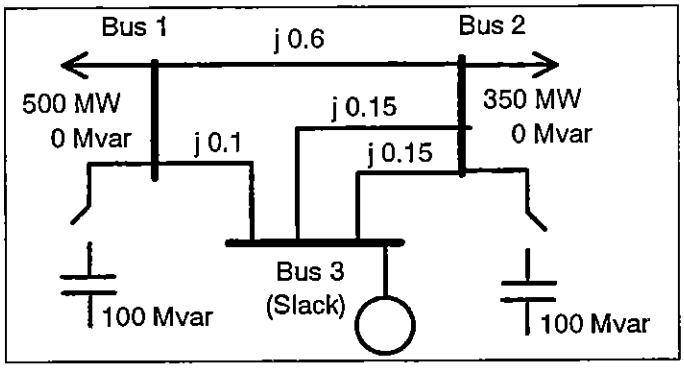

Figure 8: Three Bus System

Voltage	SEP	UEP A	UEP B	UEP C
V_1	0.952	0.560	0.747	0.574
θ_1	-31.8°	-61.0°	-44.5°	-59.7°
V_2	0.987	0.687	0.538	0.646
θ_2	-32.1°	-51.9°	-65.3°	-55.4°
$\dot{\vartheta}(x)$	--	0.297	0.274	0.297

Table 2: Three Bus System Post-Control Solutions

If $T_{p1} = T_{p2} = 2$ seconds, with no capacitor switching the system will experience voltage collapse along trajectory 1 shown in Figure 9. Note that this trajectory does not pass particularly close to either of the UEPs. Figure 10 shows the energy as a function of time. The maximum time to switch the capacitors can be estimated either from when the trajectory passes through the PEBS or when the trajectory energy is equal to that of the controlling UEP. The trajectory passes through the PEBS at about 90.5 seconds with an energy value of 0.289, which is very close to the actual maximum of 90.1 seconds (found using a series of time domain simulations). The controlling UEP could be

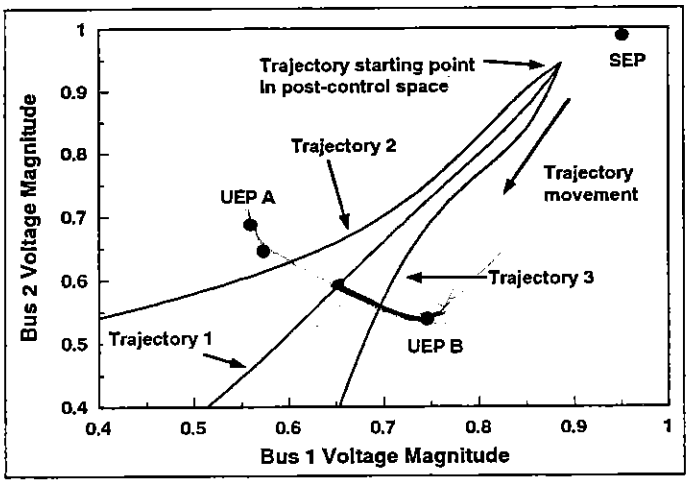

Figure 9: Three Bus Contingent System Trajectories

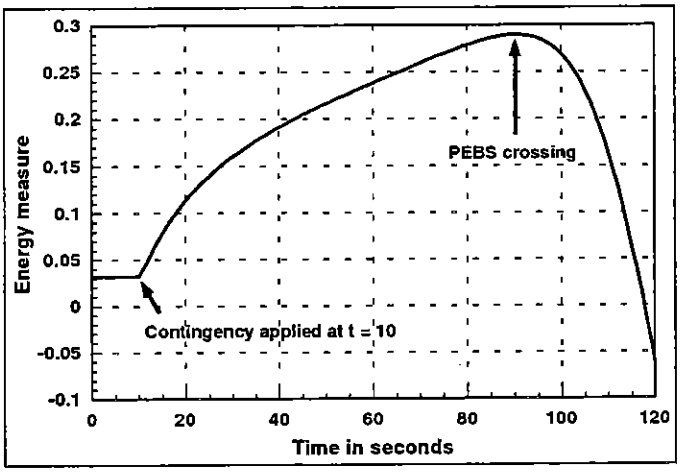

Figure 10: Trajectory 1 Energy

determined using a method similar to that of [20] of integrating the trajectory starting from the PEBS crossing point. It is also usually possible to determine this UEP by just initializing the power flow with the PEBS voltage values. Both methods indicate that UEP B is the controlling UEP. The trajectory energy value is equal to the UEP value at 77.5 seconds. Figure 11 shows the voltage recovery for a switching time slightly less than the maximum (90.0 seconds).

The dependence of the direction of voltage collapse on the load parameters is demonstrated in Figure 9 with trajectories 2 and 3. To get trajectory 2, T_{p1} was decreased to 1 second, while T_{p2} was increased to 5 seconds. The faster load recovery at bus 1 now causes that portion of the system to be more heavily loaded. Consequently, the trajectory crosses the PEBS in the vicinity of UEP A, which is now the controlling UEP. The PEBS energy of 0.297 is almost identical to that of the controlling UEP (0.296). This value is reached at about 127 seconds, which is also the actual maximum control time for this case. Conversely, for the trajectory 3 case T_{p1} was now increased to 5 second, while T_{p2} was decreased to 1

second. The faster load recovery at bus 2 now caused the trajectory to exit close to UEP B with an energy of 0.279 at 91 seconds while the controlling UEP energy level was reached at 89.8 seconds. This was also quite close to the actual of 90.8 seconds.

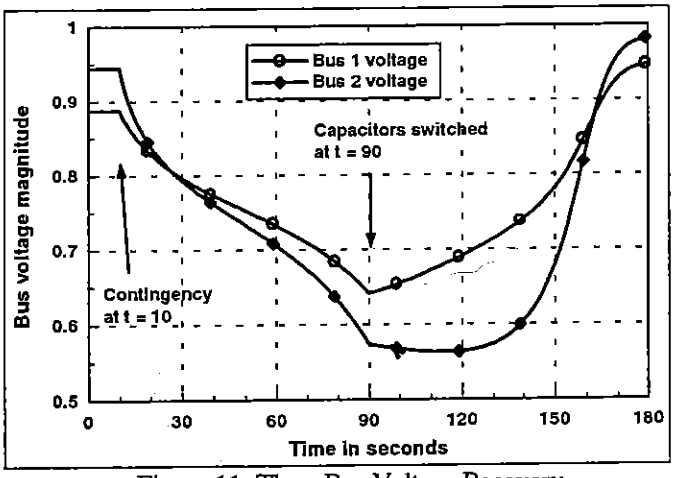

Figure 11: Three Bus Voltage Recovery

As a final example the method is demonstrated on the 118 bus case for the line 5-8 contingency. At a load of double the basecase value this contingency is unsolvable with β = 0.0648. One method (of last resort) to restore solvability is to shed load. Assume that 30 MW and 7.7 Mvar are to be shed at bus 3 (maintaining the original power factor of 0.969). The method from Section II indicates that, from a static point of view, this is sufficient to restore solvability. Again the dynamic question is to determine the maximum allowable time after the contingency to do this control. With the contingency occurring at t = 10 seconds, Figure 12 plots the energy of the system using the dynamic load models from (9) at a number of buses with $\alpha_i = \beta_i = 2$ and time constants T_{pi} & T_{qi} of 5 seconds. As was the case for the smaller systems, a sufficient condition for stability is that the load be shed before the system energy climbs to the value equal to that of the controlling UEP. For this case the UEP energy of 0.0357 is reached at 133 seconds, while the trajectory crosses the PEBS at 143 seconds with an energy of 0.0370. These values are quite close to the actual maximum of about 134.5 seconds. The controlling UEP was quickly determined by initializing a power flow solution using the PEBS crossing point values. The power flow had an initial maximum mismatch of just 0.02 per unit, and converged in 2 iterations.

The practical result of calculating the maximum allowable time frame for control application after a contingency is the determination of what controls can be used to mitigate the contingency. If the time frame is just a few seconds then either fast-acting automatic controls must be installed, or (more likely) system operation is constrained to avoid operating in that region. With a longer time frame, coupled with a plan detailing which controls to change should the contingency occur, effective intervention by the power system operator becomes a possibility. The advantage of the energy approach is that fairly good estimates of the maximum time for control application can be determined directly. Furthermore, since it is straightforward to calculate the sensitivity of the controlling UEP to various control actions [21], the energy approach could also tell which controls would be most effective in increasing this time.

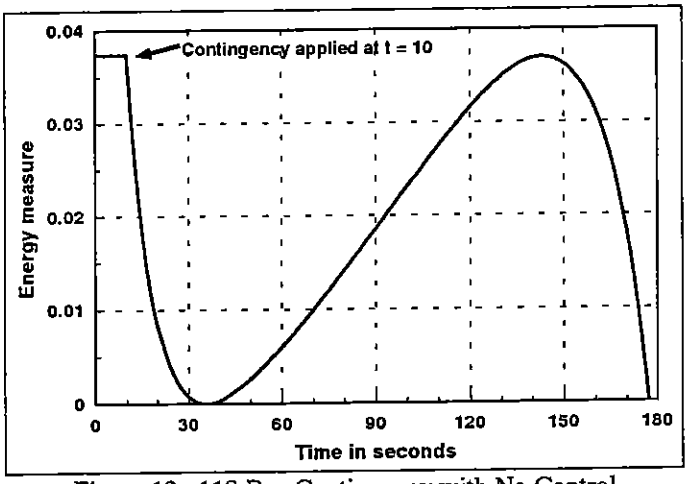

Figure 12 : 118 Bus Contingency with No Control

IV. Conclusion

This paper addresses the practical problem of power flow cases which have no real solution. It has been shown that it is straightforward to statically determine a set of controls which could restore a case to solvability. However system dynamics must also be considered to ascertain whether the controls can be applied quickly enough following the contingency to avoid voltage collapse. The paper has shown that energy methods offer the potential for directly determining the maximum allowable time frame for control application. This application of energy methods is similar to their use for the transient stability problem, with the critical energy value determined using the controlling UEP concept. Future research includes further investigation of a composite energy function suitable for both voltage and transient stability assessment, along with more detailed dynamic models.

V. Acknowledgments

The author would like to acknowledge the support of NSF through its grant NSF ECS-9209570 and the Power Affiliates program of the University of Illinois at Urbana-Champaign.

VI. References

[1] I. Dobson and H.-D. Chiang, "Towards a theory of voltage collapse in electric power systems," *Systems and Control Letters*, vol. 13, pp. 253-262, 1989.

[2] E.H. Abed and P.P. Varaiya, "Nonlinear oscillations in power systems," *Electric Power Energy Sys.*, vol. 6, pp. 37-43, Jan. 1984.

[3] T.J. Overbye, "A power flow measure for unsolvable cases," IEEE 1993 PES Summer Meeting, 93SM492-9, Vancouver, BC, July 1993.

[4] T.J. Overbye, "Computation of a practical method to restore power flow solvability," IEEE 1994 PES Winter Meeting, 94WM245-1, New York, NY, Jan. 1994.
[5] Y. Tamura, K. Iba and S. Iwamoto, "A method for finding multiple load-flow solutions for general power systems," IEEE PES Winter Meeting, A80 043-0, New York, Feb. 1980.
[6] I. Dobson, "Observations on the geometry of saddle node bifurcation and voltage collapse in electrical power systems," *IEEE Trans. on Circuits and Sys.*, vol. 39, pp. 240-243, March 1992.
[7] I. Dobson and L. Lu, "Computing an optimum direction in control space to avoid saddle node bifurcation and voltage collapse in electric power systems," *IEEE Trans. on Automatic Control*, vol. 37, pp. 1616-1620, Oct. 1992.
[8] W. Xu and Y. Mansour, "Voltage stability analysis using generic dynamic load models," *IEEE Trans. on Power Sys.*, vol. 9, pp. 479-493, Feb. 1994.
[9] K.-M. Graf, "Dynamic simulation of voltage collapse processes in EHV power systems," Proc.: Bulk Power System Voltage Phenomena-Voltage Stability and Security, EPRI EL-6183, pp. 6.45-54, Jan. 1989.
[10] M.K. Pal, "Voltage stability conditions considering load characteristics," *IEEE Trans. on Power Sys.*, vol. 7, pp. 243-249, Feb. 1992.
[11] C.W. Taylor, "Voltage stability part I: introduction, definitions, time frames/scenarios, and incidents, " Survey of the Voltage Collapse Phenomenon, NERC, pp. 51-65, Aug. 1991.
[12] D. Karlsson and D.J. Hill, "Modelling and identification of nonlinear dynamic loads in power systems," *IEEE Trans. on Power Sys.*, vol. 9, pp. 157-166, Feb. 1994.
[13] M.A. Pai, *Energy Function Analysis for Power System Stability*, Kluwer Academic Publishers, Boston, MA, 1989.
[14] A.A. Fouad and V. Vittal, *Power System Transient Stability Analysis using the Transient Energy Function Method*, Prentice Hall, 1992.
[15] C.L. DeMarco and T.J. Overbye, "An energy based security measure for assessing vulnerability to voltage collapse," *IEEE Trans. on Power Sys.*, vol. 5, pp. 419-427, May 1990.
[16] T.J. Overbye, I. Dobson and C.L. DeMarco, "Q-V curve interpretations of energy measures for voltage security," *IEEE Trans. on Power Sys.*, vol. 9, pp. 331-340, Feb. 1994.
[17] T.J. Overbye, M.A. Pai and P.W. Sauer, "Some aspects of the energy function approach to angle and voltage stability analysis in power systems," *Proc. 31th IEEE Conf. Decision and Control*, Tucson, AZ, pp. 2941-2946, Dec. 1992.
[18] T. Athay, R. Podmore and S. Virimani, "A practical method for direct analysis of transient stability," *IEEE Trans. on Power App. and Sys.*, vol. PAS-98, pp. 573-584, Mar./Apr. 1979.
[19] N. Kakimoto, Y. Ohsawa and M. Hayashi, "Transient stability analysis of electric power systems via lure-type Lyapunov function," *Trans. IEE of Japan*, vol. 98, May/June 1978.
[20] H.-D. Chiang, F.F. Wu, and P.P. Varaiya, "A BCU method for direct analysis of power system transient stability," IEEE 1991 Summer meeting, SM 423-4PWRS, San Diego, CA, July 1991.
[21] T.J. Overbye and C.L. DeMarco, "Voltage security enhancement using energy based sensitivities," *IEEE Trans. on Power Sys.*, vol. 6, pp. 1196-1202, Aug. 1991.